Earthquake Engineering, Tenth World Conference © 1992 Balkema, Rotterdam. ISBN 90 5410 060 5

Insights on 2D vs. 3D-modelling of surface foundations

J.W. Meek
Fr. Holst Construction Co., Hamburg, Germany
J.P. Wolf
Swiss Federal Institute of Technology, Lausanne, Switzerland

ABSTRACT: To simplify the analysis, 3D-soil-structure interaction problems are often modelled by considering a 2D-slice. This procedure is of questionable validity because 2D-modelling inherently overestimates the radiation damping. Valuable insights into the essence of radiation damping and the difference between 2D- and 3D-models may be obtained via approximate strength-of-materials solutions based on cone-wedge models and travel-time considerations.

1 OBJECT

To simplify the soil-structure-interaction analysis, 3-dimensional problems are often modelled by considering a 2-dimensional slice. This assumption, although convenient, is potentially dangerous because the specific radiation damping per unit contact area computed for the 2D-case overestimates the actual radiation in three dimensions. To make matters worse, 2D-modelling always entails an underestimation of the stiffness; for static loading the translational stiffness of 2D-foundation models completely vanishes. Figure 1 illustrates the unavoidable dilemma of 2D-modelling. To attain the same static rocking stiffness and the same average stiffness in horizontal translation, the 3D-disk footing with radius r_0 must be idealised by a strip footing of width 1.63 r_0 and slice length 2.54 r_0 (Luco and Hadjian (1974)). The contact area of the 2D-strip model, $A_0 = 4.14\ r_0^2$, is already 1.32 times that of the original disk and is in addition multiplied by the higher specific damping of the 2D-case. The resulting radiation dashpot computed for the strip model in translation may well exceed the actual radiation damping of the 3D-disk by over 100%. For rocking motion the error implicit in 2D-modelling is even larger.

It appears puzzling that the specific damping is larger in the 2D-case, although the opportunity for waves to spread is obviously greater in three dimensions than in two. This phenomenon has been termed a paradox (Gazetas (1984)).

The object of the present study is to provide physical insight into the damping paradox and the reduced stiffness of 2D- vs. 3D-foundations without recourse to rigourous elastodynamical solutions. Also addressed is the quite separate but related topic of the transition from square to slender rectangular foundations; such problems are solved via approximate Green's functions.

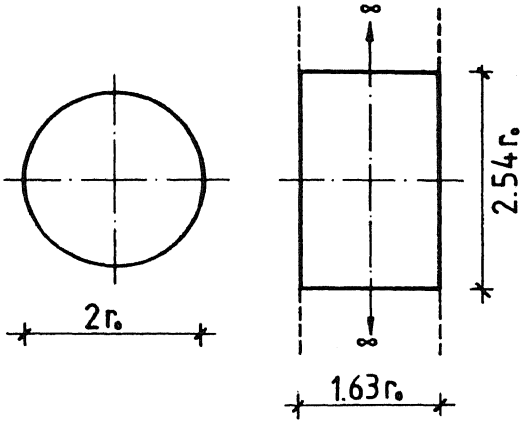

Figure 1. Disk (3D-model) and equivalent strip (2D-model).

2 METHODS AND RESULTS

2.1 *Cone-wedge model*

In lieu of the elastic halfspace with mass density ρ, the soil may be idealised by a semi-infinite cone (3D) or a wedge (2D), both for translational (Ehlers (1942)) and rotational (Meek and Veletsos (1974), Meek and Wolf (1992)) degrees of freedom. The cone or wedge with apex height z_0, depth z and surface area A_0 is shown in Figure 2. The cone or wedge experiences vertical or horizontal translation $u(z)$, the value at the surface being denoted as $u_0 = u(z_0)$. For rotational motion the same notation may be preserved if A_0 is interpreted as the moment of inertia of the foundation about its axis and u_0 is taken to be the angle of rocking or twist.

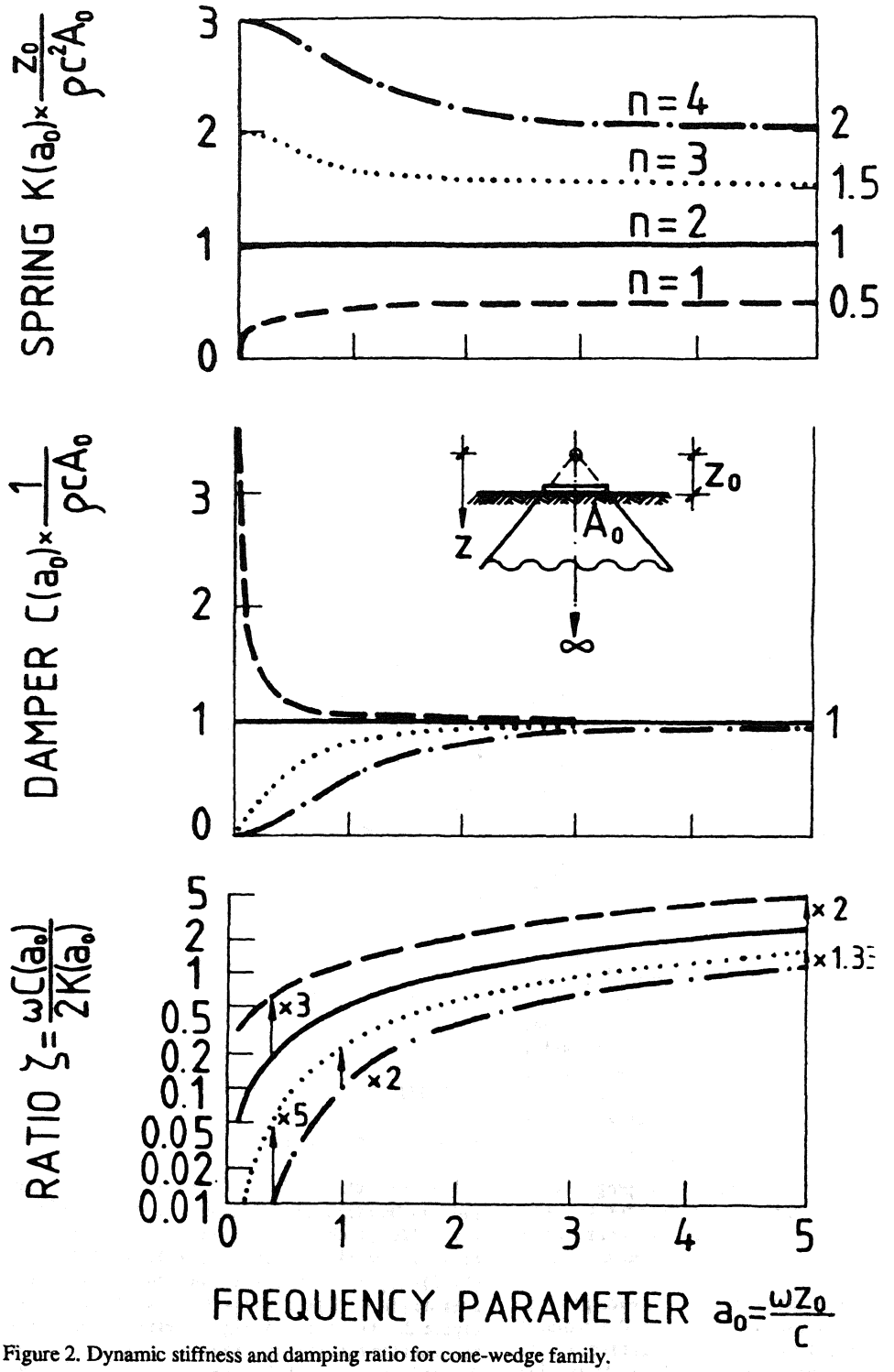

Figure 2. Dynamic stiffness and damping ratio for cone-wedge family.

For the cone-wedge family the cross section increases with depth according to the power law $A = A_0 (z/z_0)^n$. The values of the exponent n=1, 2, 3, 4 correspond in turn to the 2D-wedge in translation, the 3D-cone in translation, the 2D-wedge in rotation, and the 3D-cone in rotation. The governing equation of the cone-wedge family subjected to harmonic motion with circular frequency ω is

$$\frac{d^2u}{dz^2} + \frac{n}{z}\frac{du}{dz} + \frac{\omega^2 u}{c^2} = 0 \qquad (1)$$

in which c is the appropriate propagation velocity for the case under consideration. (For horizontal translation and torsion c = the shear-wave velocity c_s; for vertical translation and rocking c = the dilatational-wave velocity $c_p \leq 2.3\, c_s$). The propagation velocity specifies the corresponding stiffness modulus ρc^2.

In the static case ($\omega = 0$) the displacement field may be obtained by elementary integration of equation (1).

$$u = u_0 (z_0/z)^{n-1} \qquad (2)$$

The corresponding static stiffness, computed via the expression $K_0 = -\rho c^2 A_0 u_0'/u_0$, has the simple form

$$K_0 = (n\text{-}1)\, \rho c^2 A_0/z_0 \qquad (3)$$

The counterpart of the static case is the high-frequency limit $\omega \to \infty$, for which the asymptotic solution of equation (1) is given by the decaying wave

$$u = u_0 (z_0/z)^{n/2}\, e^{i\omega(z_0 - z)/c} \qquad (4)$$

Analogous to the static case, the stiffness in the high-frequency limit is again calculated via the expression $S_\infty = -\rho c^2 A_0 u_0'/u_0$

$$S_\infty = \underbrace{(n/2)\rho c^2 A_0/z_0}_{K_\infty} + \underbrace{i\omega\, \rho c A_0}_{C_\infty} \qquad (5)$$

The factor $n/2$ appearing in the spring term reflects the fact that the amplitude in equation (4) decays in proportion to $z^{-n/2}$ and not in proportion to $z^{-(n-1)}$, as in the static case. The high-frequency dashpot has the familiar specific damping (acoustic impedance) ρc, which is the same for all values of n.

For intermediate frequencies the solution of equation (1) may be written in terms of half-order Hankel functions of the second kind. The general expression for the dynamic stiffness is

$$S(a_0) = K(a_0) + i\omega C(a_0) =$$

$$\left[a_0 \frac{H^{(2)}_{\frac{n+1}{2}}(a_0)}{H^{(2)}_{\frac{n-1}{2}}(a_0)} \right] \rho c^2 A_0/z_0 \qquad (6)$$

in which a_0 denotes the frequency parameter $\omega\, z_0/c$. The dynamic stiffness $S(a_0)$ is plotted in Figure 2.

The figure shows that the static and high-frequency limits derived previously are joined by smooth curves, in the simplest case for the cone in translation (n=2) by straight lines. The asymptotic value of damping, $\rho c A_0$, is approached from above for n=1, from below for n=3 and 4. The damping of the 2D-wedge always exceeds that of the 3D-cone. (Compare the curves n=1 and 2 for translation, n=3 and 4 for rotation). The difference is especially pronounced for low-frequency translational motion; indeed, for the wedge (n=1) the damping tends to infinity in the static case. However this "infinite" damping is multiplied by "zero" frequency to obtain the imaginary part of the dynamic stiffness; and the product tends to zero.

This product is the numerator of the damping ratio $\zeta = \omega C(a_0)/(2K(a_0))$ for an oscillator consisting of a rigid foundation supported by flexible soil, the natural frequency of the coupled system being ω. The damping ratio is plotted in the bottom portion of Figure 2, which confirms that 2D-modelling significantly exaggerates the radiation damping, usually by more than 100% as specified by the multipliers in the figure. In the formula for the damping ratio the 2D-effects (increased damping in the numerator, reduced stiffness in the denominator) compound one another.

If the governing equation (1) for the cone-wedge family is non-dimensionalised, the independent depth variable z is replaced by $\omega z/c$. Thus the high-frequency case $\omega \to \infty$ corresponds just as well to the far-field case $z \to \infty$. The asymptotic solution equation (4) therefore also describes the behaviour "at infinity". Here conservation of energy requires that the amplitude decays in inverse proportion to the square root of the area, in agreement with the exponent $n/2$ in equation (4) (Meek and Wolf(1991)). If the exponent n–1 for the near-field static solution (equation (2)) happens to be identical to the exponent $n/2$ for the far field, as is the case only for the translational cone (n=2), the distinction between the near and the far field vanishes; and radiation energy is transferred smoothly for all frequencies: The result is constant frequency-independent damping as shown in Figure 2. By contrast, if n–1 is greater than $n/2$, as is the case for rotation (n=3 or 4), the static displacement will have died off to a small value at the beginning of the far field. For low frequencies very little energy will reach the far-field boundary and penetrate to infinity: The damping begins at zero (Figure 2). With increasing frequency the far-field boundary is pulled in towards the foundation, and the damping gradually increases. Just the opposite occurs for the wedge in translation (n=1). According to the exponent n–1=0, the static amplitude arrives undiminished at the beginning of the far field. For low frequencies there is a very pronounced tendency to radiate, which leads to infinite damping in the limit $\omega \to 0$. The essence of radiation damping must be grasped in this fashion. The heuristic concept of more spreading of waves in three dimensions than in two is misleading. Indeed, just the opposite is true: The less the amplitude spreads and diminishes with distance, the greater is the radiation damping.

2.2 *Row of point loads*

The cone-wedge model, while quite simple, requires the solution of a differential equation. The salient features of 2D- translational behaviour may also be derived purely on the basis of travel-time considerations referred to a row of identical point loads (separated by the distance b) (Figure 3). For static and low-frequency dynamic motion the vertical displacement of the surface of the halfspace due to a single point load decays in inverse proportion to the horizontal distance from the source. If c denotes the horizontal velocity of wave propagation in the near field (somewhat less than the Rayleigh-wave velocity), the displacement at time t due to an infinite array of point loads is

$$u(t) = 2\,\frac{1-\upsilon}{2\pi G}\sum_{n=0}^{\infty}\frac{P\,[t-(n+1/2)\,b/c]}{(n+1/2)\,b} \qquad (7)$$

The leading factor 2 accounts for the left and right semi-infinite rows of loads, and the constant $(1-\upsilon)/(2\pi G)$ is obtained from the static Boussinesq solution for an elastic material with shear modulus G and Poisson's ratio υ. For harmonic motion the Fourier transform of equation (7) yields

$$u = 2\,\frac{(1-\upsilon)\,P}{2\pi G b}\sum_{n=0}^{\infty}\frac{e^{-i\omega(n+1/2)b/c}}{n+1/2} \qquad (8)$$

The sums for the real and imaginary parts of equation (8) may be evaluated explicitly (Jolley (1961), series N° 549 and 550). The resulting expression for the dynamic stiffness $= P/u$ is

$$S(a_0) = \frac{\pi G b}{1-\upsilon}\,[k(a_0) + i a_0\, c(a_0)] \qquad (9)$$

with $a_0 = \omega b/c$. The spring and damping coefficients

$$k(a_0) = \frac{\ln\cot(a_0/4)}{[\ln\cot(a_0/4)]^2 + \pi^2/4} \qquad (10)$$

$$c(a_0) = \frac{\pi/(2a_0)}{[\ln\cot(a_0/4)]^2 + \pi^2/4} \qquad (11)$$

are plotted in Figure 3. For the low-frequency range $a_0<1$ the response is essentially identical to that of the translational wedge ($n=1$ in Figure 2). The static stiffness is zero but the spring coefficient increases abruptly to a more or less constant value. By contrast, the damping coefficient begins from infinity and then diminishes asymptotically. For $a_0>1$ the spring coefficient gradually decays, reaching zero when $a_0=\pi$. This is a resonant condition, in which the distance b between point loads is half a wavelength.

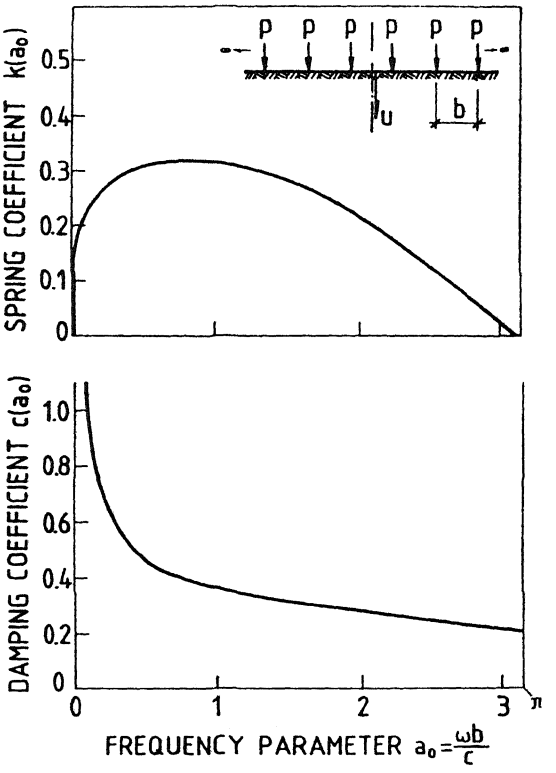

Figure 3. Dynamic-stiffness coefficient for row of point loads.

2.3 *Approximate Green's function*

If the point load is replaced by a small disk with finite diameter, travel-time considerations analogous to equation (7) enable modelling of surface foundations with arbitrary shape. For better accuracy, the displacement, which decays in inverse proportion to the distance in the near field as above, is modified to decay in inverse proportion to the square root of the distance in the far field (Rayleigh waves). If a rectangular foundation with width $2b$ and length $2a$ is idealised by an array of small subdisks, the spring and damping coefficients shown in Figure 4 for vertical motion are calculated for various slenderness ratios a/b. The curves correspond to the conventional representation of the dynamic stiffness in the form

$$S(a_0) = K_0\,[k(a_0) + i a_0\, c(a_0)] \qquad (12)$$

in which K_0 is the static stiffness and a_0 is the dimensionless frequency $\omega b/c_s$. These results computed using the approximate Green's function described above are in excellent agreement with rigorous elastodynamical solutions.

At first glance it would appear that as the foundation becomes more slender and tends toward the 2D-strip,

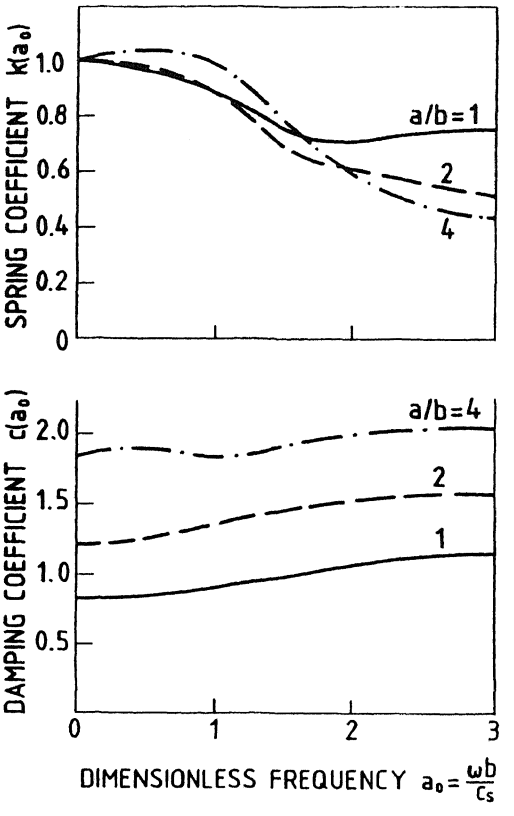

Figure 4. Dynamic-stiffness coefficients for rectangular foundations.

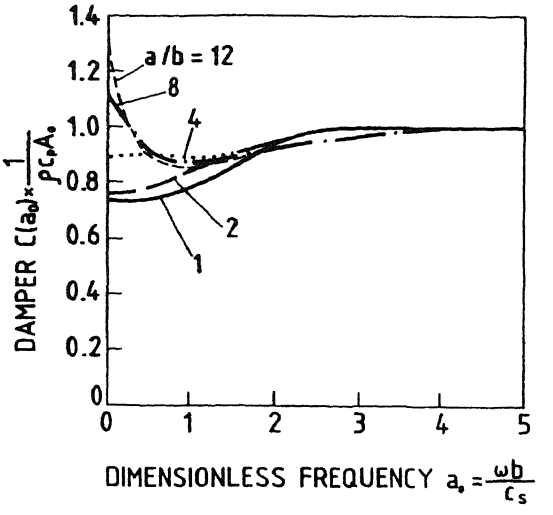

Figure 5. Frequency-dependent damper for vertical motion of rectangular foundations.

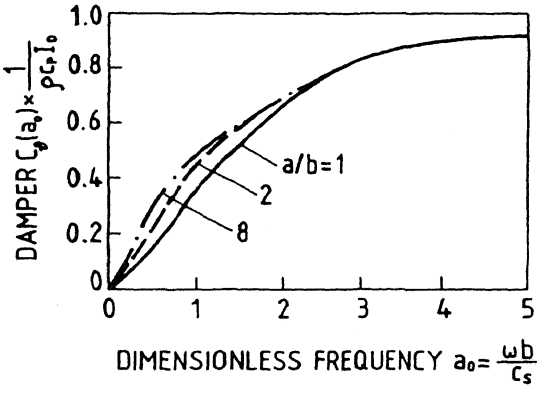

Figure 6. Frequency-dependent damper for rocking motion of rectangular foundations.

the damping increases enormously. However, the major portion of the apparent increase in damping is associated with the definition of a_0 in terms of the foundation's halfwidth b. Instead of the conventional expression for the imaginary portion of the dynamic stiffness, $K_0 a_0\, c(a_0)$, it is physically more meaningful to use the characteristic impedance for vertical motion ρc_p and write the imaginary part as $\omega C(a_0)$. The ratio $C(a_0) / (\rho c_p A_0)$ is shown in Figure 5. In the low-frequency range the specific damping does increase with the slenderness ratio; however, the effect is not very pronounced and is even less appreciable for the rocking case, Figure 6.

The static stiffness of rectangular foundations is compared to that of a disk with same area A_0 (translation) or the same moment of inertia I_0 (rotation) in Figure 7. Due to the increased corner-punching effect, the rectangular footing is always stiffer than the equivalent disk; and the stiffness ratio increases with the slenderness ratio. This seems to contradict the fact that the 2D-strip is softer than the 3D-disk.

However, no paradox is involved. The static stiffness in Figure 7 is computed with respect to the total load on the rectangular foundation, not the load per unit length, which is the reference quantity for the 2D-strip. If Figure 7 were to be redrawn on a per-unit-length basis, the rectangular foundation would appear to be more flexible than the disk.

By use of Figure 7 to modify the static stiffness, it is possible to replace rectangular foundations by equivalent disks in order to facilitate the dynamic analysis. As demonstrated by Figures 5 and 6, the resulting error in the radiation damping is rather small. These observations indicate that it is better to simplify a complicated soil-structure interaction problem by reducing it to a radially-symmetric 3D-model instead of a 2D-slice. The authors concur with Luco and Hadjian (1974) that 2D-modelling cannot be recommended for actual engineering applications.

3 CONCLUSIONS

The salient aspects of 2D-modelling of a foundation-

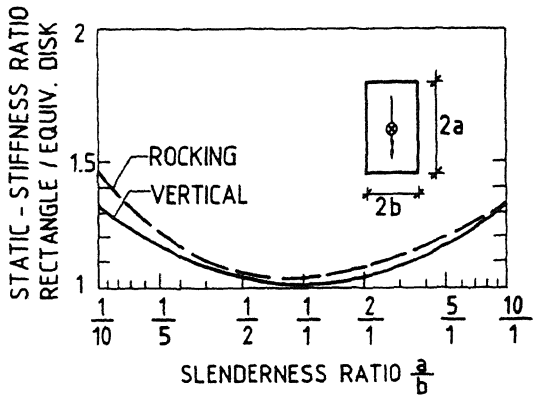

Figure 7. Static-stiffness ratio of rectangular foundation to equivalent disk.

dynamics problem are the increased damping and reduced stiffness of the 2D-idealisation by comparison to the actual 3D-case. Valuable insights into both effects, which compound one another, may be obtained via approximate strength-of-materials methods based either on cone-wedge models or travel-time considerations. The greater opportunity for wave spreading in three dimensions than in two dimensions does not lead to increased radiation damping. Rather, just the opposite is true. The more slowly the amplitude spreads and diminishes with distance from the source, the greater is the energy transmission through the far-field boundary towards infinity. Because the damping ratio is grossly overestimated, 2D-modelling cannot be recommended for actual engineering applications. It is more feasible to take the opposite approach and idealise slender soil-structure interaction problems with a radially-symmetric model. Rectangular foundations are slightly less flexible than equivalent disk footings; this effect may be accounted for via a simple correction factor applied to the static stiffness. The radiation damping of rectangular foundations with aspect ratios $a/b < 4$ does not deviate appreciably from that of the equivalent disk.

REFERENCES

Ehlers., G. 1942. The effect of soil flexibility on vibrating systems. *Beton und Eisen* 41: 197-203 (in German).

Gazetas, G. 1984. Simple physical methods for foundation impedances (*Developments in soil mechanics and foundation engineering*, Vol. 3). P.K. Banerjee and R.Butterfield Eds. London: Elsevier.

Jolley, L.B.W. 1961. *Summation of Series*. New York: Dover.

Luco, J.E. & Hadjian, A.H. 1974. Two-dimensional approximations to the three-dimensional soil-structure interaction problem, *Nuclear Engineering and Design* 31: 195-203.

Meek, J.W. & Wolf, J.P. 1991. Insights on cutoff frequency for foundation on soil layer. *Earthquake Engineering and Structural Dynamics* 20: 651-665.

Meek, J.W. and Wolf, J.P. 1992. Cone Models for Homogeneous Soil. *Journal Geotechnical Engineering Division*, ASCE 118: May.

Meek, J.W. & Veletsos, A.S. 1974. Simple models for foundations in lateral and rocking motion. *Proceedings of the 5th World Conference on Earthquake Engineering*, Vol. 2 : 2610-2613. Rome: IAEE.